

A spatial and temporal analysis of mangroves vegetation of The Gambia using seasonal metrics derived from times series of remotely sensed data in Earth Engine

Issoufou Liman Harou^{1,2*}, Julliet Inyele³, Lalisa Duguma¹

¹ Governance and Landscapes, World Agroforestry (ICRAF), Nairobi, Nairobi, Kenya

² Department of Environmental Sciences, Kenyatta University, Nairobi, Nairobi, Kenya

³ Department of Geography, Kenyatta University, Nairobi, Nairobi, Kenya

Correspondence*:

Issoufou Liman Harou

issoufoul@gmail.com

2 ABSTRACT

Gambia, relative to its size, has an extensive mangrove cover along its coast. This unique vegetation serves numerous roles. It is the source of edible products sourcing (e.g., shellfishing) for thousands of households living close to the water systems. The vegetation is also the source of wood for energy, construction and other household utensils and farm materials. Of late, there is a lot ongoing in the mangrove ecosystems and the spatial coverage of this vegetation type has been oscillating between gains and losses. A proper account of change magnitude and where the changes have been happening is not widely studied. In some case, the methods deployed even may have uncertainties that made the estimates to vary between studies. We estimated the spatial-temporal dynamics of mangrove between 2000 and 2020. We used 2,916 Landsat and 959 MODIS tiles (used for filling gaps in Landsat data) of land surface reflectance data spread across 3 bands (i.e., visible red, near infrared and shortest wave infrared) acquired between the years 2000 and 2020. The atmospherically corrected Landsat and MODIS surface reflectance provide reasonable estimates of target reflectance as it would be measured on the ground, making them good candidates for land use and land cover analysis. A classification accuracy of 0.97 and above was achieved both for the overall accuracy and Kappa coefficient. The results revealed that mangroves in The Gambia made net gains over the time period considered. Mangroves, in general, made a significant gain with a net area gain of about 7,784 ha over the 20 years period. The total area gain of mangroves in the period was about 11,951 ha (with almost 598 ha per year). During the same period, the loss in the existing mangrove vegetation area was estimated to be 4,167 ha with an estimated annual loss of about 208 ha. This observed recovery of the mangrove extent could largely be attributed to growing awareness about the importance of this vegetation type for coastal area resilience and the livelihoods of thousands who depend on it. We, however, want to note that the observed net gains should not mask the ongoing degradation of mangroves in other parts of the country. With the losses of such, the damage to livelihoods and biodiversity such as fish and marine life is significant. There

28 still needs a strong push for minimizing the losses being recorded and invest in restoring those
29 areas that are devoid of the vegetation already.

30 **Keywords:** Satellite image time series; Landsat data; Land cover classification; Change detection; Mangrove; Google Earth Engine

INTRODUCTION

31 The Gambian mangroves, extending up to 160 km from the coast along the River Gambia and covering
32 an area ranging between 497 and 747 km², are among the most developed mangroves of West Africa
33 (Ajonina et al., 2013; Feka and Ajonina, 2011; Spalding et al., 1997). In The Gambia, mangroves provide
34 fish, oysters, shrimps, wood fuel, and timber for construction along with many other ecosystem services
35 to the coastal inhabitants (Ceesay et al., 2017; Satyanarayana et al., 2012; UNEP, 2007). There is a need to
36 monitor the use of these mangroves for sustained provisioning of the services they provide (Satyanarayana
37 et al., 2012).

38 Despite the importance of these ecosystems for the Gambian communities, the current trend of
39 mangroves vegetation in The Gambia remains unclear. The interpretations of mangroves dynamics in
40 the region diverge because the scale of most remote sensing analysis do not always capture local accounts
41 of destruction (Fent et al., 2019). Spalding et al. (1997) reported a decrease from 600 to less than 500
42 km² between 1982 and 1995. UNEP (2007) reported a slight decrease in mangroves vegetation and
43 attributed it to drought, increase in soil salinity, illegal exploitation and land use conversion. Ceesay et al.
44 (2017) estimated this decline in Tanbi Wetlands National Park of The Gambia at 6% between 1973 and
45 2012 and attributed it to increase salinity which negatively affect mangrove regrowth and rejuvenation. In
46 Central River region of The Gambia, Ali Bah (2019) estimated this decline at 5.54% between 1984 and
47 1994, 7.18% between 1994 and 2007 and 22.02% between 2007 and 2017 and attributed it to increase
48 temperature and decrease in rainfall. In contrast, Fent et al. (2019) found an overall increases in
49 mangrove vegetation areas of 51.21% between 1988 and 2018 across The Gambia and in the Sine Saloum
50 and lower Casamance estuaries in Senegal. In these areas, mangroves have seen important recovery
51 between 1988 and 1999 following the increased precipitation and tree species regrowth that experiences
52 diebacks due to salinisation caused by drought (Fent et al., 2019). It is clear from these studies that
53 mangroves dynamics is a complex topic that require multi-disciplinary approaches where various scale-
54 dependent factors are required. Evidence from recent studies (Fent et al., 2019) have shown that neither
55 climatic, nor political, nor anthropogenic factors alone can explain the dynamic of mangroves vegetation
56 near the Gambia, and arguably elsewhere. While Sine Saloum experienced lower precipitation increase
57 between 1988 and 1999 compare to Low Casamance, the former have seen an important increase and the
58 latter a slight decline in mangrove vegetation (Fent et al., 2019).

59 Perhaps, the reasons for these discrepancies in estimates can be explained by the sporadic nature of the
60 available studies which targeted different period and scale of analysis. In our knowledge, none of these
61 studies succeeded in fully reconstructing the time series of satellite images due to various remote sensing
62 artifacts in the region and limitations in computing resources for handling big data. With few exceptions
63 (Fent et al., 2019), studies aiming at The Gambian mangroves have not been sufficiently holistic in the
64 sense of explaining the dynamics of the biophysical settings in their specific context. Most the available
65 estimates of mangroves areas and trends in The Gambia used single point images classification approaches
66 in an image differencing framework. Many problems can arise. Because mangroves can be easily confused
67 with other ecological systems (e.g. forests), studies aiming to provide realistic estimates of mangroves
68 dynamics should accurately account for spatial and temporal variability of coastal ecosystems (Fent et al.,
69 2019).

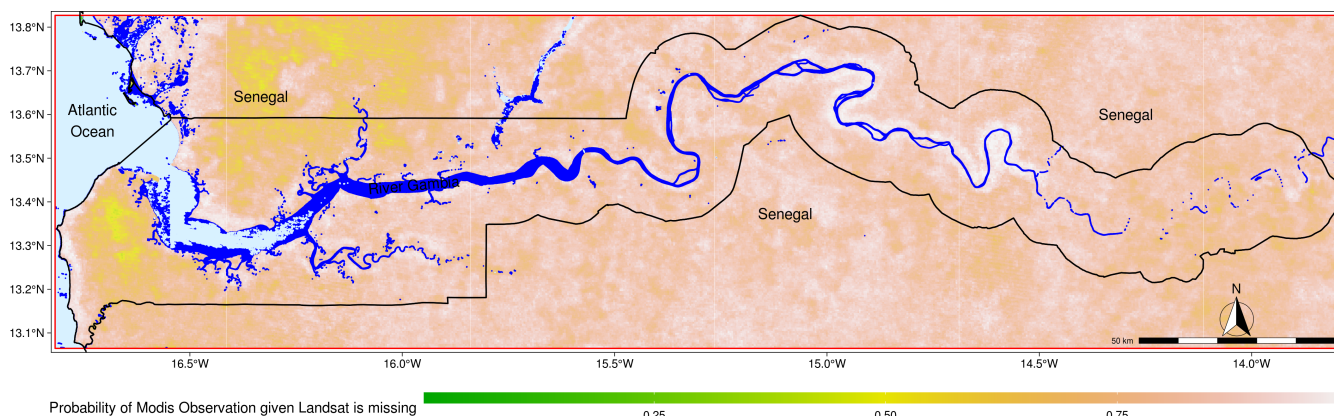


Figure 1. Delineating the referential area for the analysis.

70 The objective of this study is to assess mangrove extent dynamics in The Gambia. We used locally
 71 continuous time series of remotely sensed images to map all major land use and land cover (LULC) while
 72 putting emphasis on mangrove vegetation dynamics in the Gambia.

MATERIALS AND METHODS

73 0.1 Definition of key terms

74 In this section, we define several terms which may lead to confusion. Remote sensing artifacts regroup
 75 all atmospheric (e.g., such as cloud, cloud shadow, haze, aerosol scattering) and technical factors (e.g.,
 76 scan line corrector failure in Landsat 7 Enhanced Thematic Mapper Plus) that would potentially lead to
 77 unrealistic pixel value estimates. The term “clear” (as in clear pixels or clear observation) is meant for
 78 pixels exempt of any remote sensing artifacts. We used the term “cloudy” (as in cloudy observations or
 79 cloudy pixels) to denote pixel value identified by Fmask algorithm as affected by remote sensing artifacts.
 80 These are different from “noisy” (as in noisy observations) which are to be understood as clear pixel whose
 81 values are not reasonably within the range of valid values. These are mostly cloudy pixels not identified
 82 by Fmask algorithm. We used the term “signal” to denote the smooth temporal distribution of pixel values
 83 that describes the average phenological profile at the pixel. This is the information of interest as opposed
 84 to “noise” which denotes the random fluctuations that obscures the signal.

85 0.2 Study area

86 The study area, The Gambia (Figure 1), is located on the Gulf of Guinea, bordered by the Atlantic Ocean
 87 to west while forming an enclave within Senegal. The country occupies an area of 10,689 km² extending
 88 320 km along Gambia river. As of 2013, the population of The Gambia is estimated at 1.9 million with
 89 a growth rate of 3.3% per annum (The Gambia Bureau of Statistics, 2012). The prevailing climate is of
 90 type Sudan Sahelian with an average annual rainfall of around 900 mm, a mean temperature near 25°C,
 91 a long dry season between November to May and a rainy season between June to October. Gambia river
 92 is perhaps the most visible feature of The Gambia with its densely continuous tickets of mangroves that
 93 represent a valuable shelter for diverse species (Spalding et al., 1997).

94 For reference data, we considered the rectangular area enclosing the country to include all mangroves.
 95 The Gambian mangroves have been the center of important debates - mangrove regrowth versus
 96 mangroves degradation - over the last few decades. The Gambia has a reach body of LULC (e.g., water
 97 bodies, forests, savannas, shrublands, croplands), most of which are strongly influenced by the prevailing
 98 anthropogenic and ecological processes taking place in the coastal regions (Andrieu, 2018).

0.4 Referential for data and image classification

110 We conducted extensive field survey to systematically collect reference data for training and validation
111 of LULC classification. These training and validation polygons, collected following the guidelines and
112 class definition of the international geosphere–biosphere program (IPB, 2009) and the FAO Land cover
113 Classification System (Di Gregorio et al., 2016), are fairly evenly distributed across the major LULC
114 platform (Gorelick et al., 2017; Vermote et al., 2019). These reference periods account for 2916 Landsat
115 and 959 MODIS tiles (used for filling gaps in Landsat data) of land surface reflectance data spread across
116 LULC classification. Considering that land use and cover change in the study areas are mostly gradual and
117 sloping (i.e. visible red, near infrared and shortest wave infrared) acquired between the years 2000
118 and 2020. The atmospherically corrected Landsat and MODIS surface reflectance provide reasonable
119 estimates of target reflectance as it would be measured on the ground, making them good candidates for
120 LULC analysis. The main artifact that influences the usefulness and usability of these images in the study
121 area is the important cloud coverage during the rainy season. By considering multiple years, hence deriving land use and cover classification over a period, we minimized
the chances of capturing noise, because LULC changes due to noise tend to be ephemeral whereas true
land cover changes tend to persist through time (Zhu and Woodcock, 2014).

122 To account for the spatial distribution of LULC in relation to the reflectance values in the image time
123 series, we constrained the training and validation data to areas whose classes have not changed between
124 the reference periods, given the spatial and temporal distribution of the surface reflectance values. We
125 used k means clustering to produce unsupervised classifications (15 classes distributed over 1000 random
126 points) for both reference periods based on which we conducted a stratified random sampling across those
127 locations whose LULC remain unchanged. This required careful visual observation and matching of class
128 configurations across the entire landscapes of the classified images. While this process was tedious and
129 time consuming, it helped us to produce classifiers that are consistent with both reference periods. For
130 each class (Table 1), we considered 500 samples, making a total of 7500 points, to train and validate a
131 model for land use and land cover classification.

Table 1. Categories of land use and land cover used for an image classification in The Gambia.

Standard class	Class description	Map legend
Fresh water	Lakes, rivers, and other reservoirs that are dominantly freshwater bodies.	Fresh waters
Salty water	Oceans, seas and other reservoirs that are dominantly salty water bodies.	Salty waters
Closed forests	Lands dominated by trees with a percent cover greater than 70 % during the entire period of the year.	Closed forests
Open forests	Lands dominated by trees with a percent cover between 60 and 70 % during the entire period of the year.	Open forests
Woody savannas	Lands with herbaceous and other understory systems, and with forest canopy cover between 30% and 60%. The forest cover height exceeds 2 m.	Woody savannas
Savannas	Lands with herbaceous and other understory systems, and with forest canopy cover between 10% and 30%. The forest cover height exceeds 2 m.	Savannas
Closed shrublands	Lands with woody vegetation less than 2 m tall and with shrub canopy cover > 60%. The shrub foliage can be either evergreen or deciduous.	Closed shrublands
Open shrublands	Lands with woody vegetation less than 2 m tall and with shrub canopy cover between 10% and 60%. The shrub foliage can be either evergreen or deciduous.	Open shrublands
Grasslands	Lands with herbaceous types of cover. Tree and shrub cover is less than 10%.	Grasslands
Permanent wetlands	Lands with a permanent mixture of fresh water and herbaceous or woody vegetation.	Wetlands
Croplands	Lands covered with temporary crops followed by harvest and a bare soil period (e.g., single and multiple cropping systems). Perennial woody crops are classified as the appropriate forest or shrub land cover type.	Croplands
Urban and built-up lands	Land covered by buildings and other man-made structures.	Built-up
Cropland / natural vegetation mosaics	Lands with a mosaic of croplands, forests, shrubland, and grasslands in which no one component comprises more than 60% of the landscape.	Mosaics
Barren	Lands with exposed soil, sand, rocks, or snow and never have more than 10% vegetated cover during any time of the year.	Barren
Mangroves	Lands with a permanent mixture of salty or brackish water and herbaceous or woody vegetation.	Mangroves
Regularly Flooded Vegetation	Land transitioning between terrestrial and fresh water zones with sufficient moisture for the development of near evergreen vegetation.	Riparian Vegetation

Note:

Fresh and salty water, based on the definition of class water bodies in IGBP land cover classification system, are considered to capture the reach of fresh and salty water as this can be relevant in the context of mangrove ecosystems. Closed and opened forests are based on FAO LULC classification system. The remaining class are based on IGBP land cover classification system.

132 This study involved a systematic review of the existing literature aimed to mangrove ecosystems in The
 133 Gambia and neighboring areas as well as a remote sensing-based analysis of mangroves change using
 134 continuous time series. Our approach for change detection unravels several mysteries surrounding the
 135 topic to address several shortcomings regarding LULC analysis in The Gambia and can provide clues for
 136 accurate LULC analysis elsewhere. It involved several steps for data scaling and gaps filling to minimize
 137 the effects of sensors difference (e.g., Landsat ETM+ versus Landsat OLI) and remote sensing artifacts
 138 (e.g., clouds, and cloud shadows) along with a temporal smoothing to remove random noise.

139 0.5 Image pre-processing

140 As mentioned earlier, we used the geometrically and atmospherically corrected Landsat surface
 141 reflectance products. These products are provided along with a quality assessment band which we used
 142 to mask all pixels affected by remote sensing artifacts. Although these are currently amongst the best
 143 available Landsat and MODIS products in the public domain, they often need to be further processed
 144 prior to analysis involving continuous observations. Since the atmosphere correction may fail to account
 145 for these remote sensing artifacts (Zhu and Woodcock, 2014), we discarded all pixels but those acquired
 146 under clear conditions. In the few cases where no clear acquisition is available, we created an empty
 147 image to keep track of missing data and provide a slot for gap filling, which we conducted in 3 steps. Roy
 148 et al. Roy et al. (2016) noted differences between OLI and others Landsat data and provided coefficients
 149 for harmonizing these using linear transformation. We scaled all data from other sensors to OLI, so that
 150 the time series can be comparable over the 20 years. This is particularly important for studies using water
 151 or vegetation indices because the difference is higher in the near infrared and short wave infrared bands
 152 whereas atmospheric correction increases this difference in the visible bands (Roy et al., 2016).

153 The first step for gap filling consisted in computing the monthly median composites, considering a lag
 154 of 31 days. This reduced the number of images to 12 medians images per year, corresponding to 1 image
 155 per month. The median has proven to be a robust statistic in the sense that it is tolerant to outliers and
 156 noisy observations.

157 In the second step, we used the median of the corresponding MODIS acquisition of the month to fill data
 158 gaps in the Landsat composite where these MODIS data are available. We then computed the normalized
 159 difference vegetation (NDVI) and water (NDWI) indices, which we used for subsequent analysis. The
 160 use of these indices can also improve the accuracy in data estimates since values beyond the range [-1, 1]
 161 are systematically discarded. The choice of these two spectral indices is motivated by their sensitivity to
 162 water and vegetation, which are sufficient to describe the landscape of the study area when times series
 163 are available. The third step exploit the vegetation and water seasonality in the study region, hence the

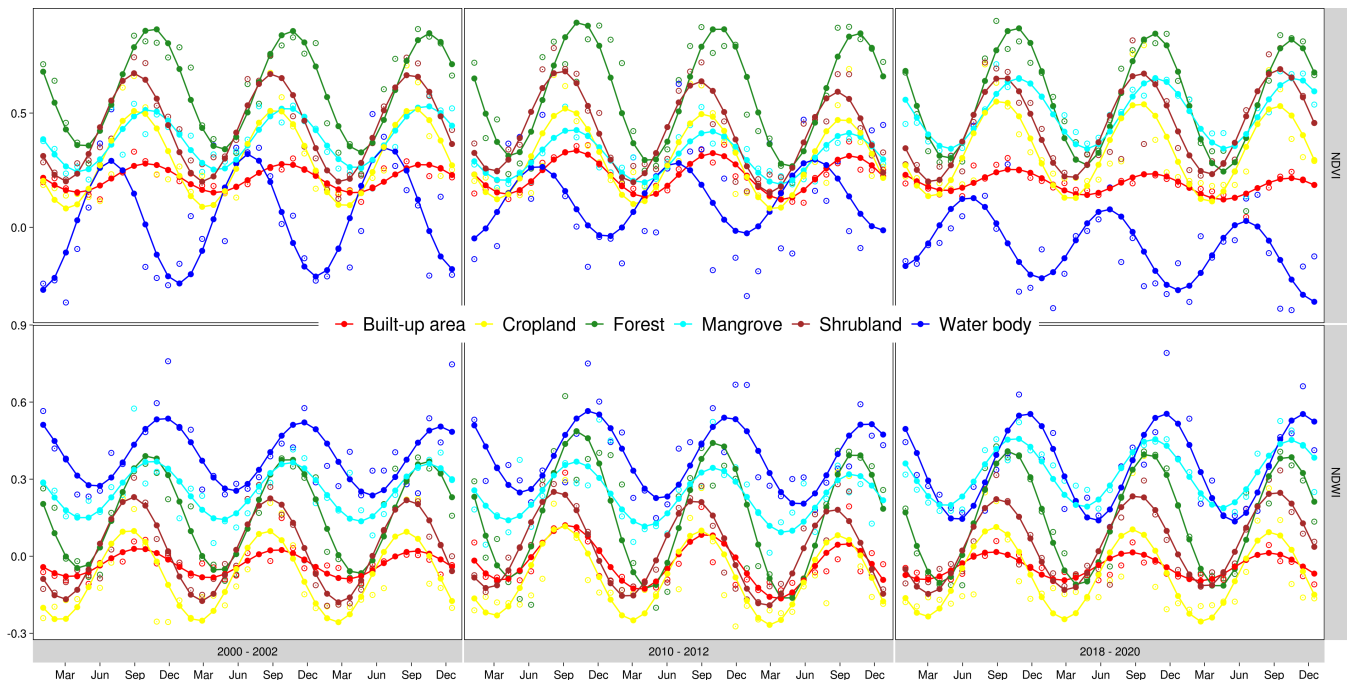


Figure 2. Available monthly median Landsat NDVI and NDWI values after MODIS gap filling (red points), and their corresponding predicted values (green lines) estimated using harmonic modelling at different location in The Gambia. This figure illustrates how the model fits to different data inputs to capture variations across multiple pixels.

164 temporal relationships between consecutive observations captured in the time series, to infer missing data
 165 using harmonic modelling. Many realistic models for time series analysis assume a component describing
 166 a consistent signal and another component representing random noise (Shumway and Stoffer, 2011). This
 167 is consistent with the behaviors of most ecological systems, particularly in the study area. We adopted
 168 the harmonic modelling approach to minimize the effects of such noise which are mere representation
 169 of ephemeral variability. Under these considerations, we described pixel values as random variables
 170 chronologically indexed by time.

171 Many problems in the frequency domain of time series analysis can be express as local, polynomials
 172 and splines regression using linear models (Shumway and Stoffer, 2011). In situation where trend is of
 173 interest, the time series can be described using a linear regression model that predicts the pixel values
 174 based on time (equation 2).

Let

p_t be the pixel value at time t

$t = t_0, t_1, \dots, t_N$ be the time indices

Then,

$$p_t = \beta_0 + \beta_1 t + e_t$$

Where,

β_0 is the intercept of the regression line

β_1 is the slope of the regression line

e_t is the random noise

p_t is the predicted pixel value at time t

(1)

175 In situation where the periodic component is of interest, as it is the case in our study region, linear
 176 regression can still accurately recover the periodic signal using sines and cosines as inputs (Shumway
 177 and Stoffer, 2011; Zhu and Woodcock, 2014). To accurately represent the prevailing seasonal variation
 178 in water and vegetation in the study region, we adopted a non-linear model with a sinusoidal waveform
 179 (equation 1; Non-linear form) which we linearized (equation 1; Linearized form) to fit local ordinary least
 180 squares regression (OLS) models that predict the NDVI and the NDWI based on time. For each pixel, we
 181 considered one cycle a year, corresponding to the single rainy season in the study area, to compute the
 182 OLS coefficients and fully specify the model which we then used to fill the remaining gaps in the original
 183 time series (Figure 2). We adopted the same harmonic modelling approach on the gap-free time series to
 184 remove random noises and recover the main signal which we used as input for subsequent analysis.

$$\begin{aligned}
 p_t &= \beta_0 + \beta_1 t + A \cos(2\pi\omega t + \varphi) + e_t && (\text{Non-linear form}) \\
 &= \beta_0 + \beta_1 t + \beta_2 \cos(2\pi\omega t) + \beta_3 \sin(2\pi\omega t) + e_t && (\text{Linearized form})
 \end{aligned}$$

Where,

- β_0 is the intercept (Starting point of p)
- β_1 is the slope (How fast p changes with time)
- t is the time indexed at t_0, t_1, t_N (Time since the epoch in radians)
- A is the amplitude (The peak)
- ω is frequency of oscillation ($\omega = 1$ for a single cycle)
- φ is a phase shift (Time at which p reaches its peak)
- $\beta_1 t$ is then, the linear term (Inter-annual variability)
- $A \cos(2\pi\omega t + \varphi)$ is then, the harmonic term (Main signal as sinusoidal waveform)
- e_t is the random noise
- p_t is the predicted pixel value at time t
- β_2, β_3 are the harmonic coefficients (Intra-annual variability)

With,

$$\begin{aligned}
 \beta_2 &= A \cos(\varphi) \\
 \beta_3 &= -A \sin(\varphi) \\
 A &= (\beta_2^2 + \beta_3^2)^{\frac{1}{2}} \\
 \varphi &= \tan^{-1} \frac{\beta_3}{\beta_2} \\
 A \cos(2\pi\omega t + \varphi) &= \beta_2 \cos(2\pi\omega t) + \beta_3 \sin(2\pi\omega t)
 \end{aligned} \tag{2}$$

185 0.6 Land use and land cover analysis and accuracy assessment

186 The preprocessed data for image classification consisted of 76 monthly images for each reference period,
 187 with 36 bands for each of NDVI and NDWI. To provide comprehensive accuracy assessments, we split
 188 the 7500 reference data points collected into 20% for training and 80% for validation. For each reference
 189 period, we trained and validated a random forest classifier considering a maximum number of 100 trees.
 190 The accuracies of the 3 models are almost identical that we did not preferred one over another. Instead, we
 191 used each model to classify the image based on which the model was derived. It is important to note that
 192 classifications aiming to accurately detect LULC change, as in the case of images differencing, should
 193 use classifiers that are comparable in regard to their throughputs, or at least a single model to ensure the
 194 comparability of the results.

195 0.7 Land use and land cover change analysis

196 LULC change analysis include both qualitative and quantitative analysis of changes. The qualitative part
 197 consisted in examining the areas where changes have occurred using image differencing involving 2000-
 198 classification, 2010-classification and 2020-classification. The quantitative analysis estimated the areas
 199 fluctuating between the major LULC considered.

200 To provide a complete picture of the landscape, we estimated the dynamics across all the major
 201 LULC. We then focused on mangrove vegetation where we detected changes in mangrove vegetation
 202 by comparing LULC over areas detected as mangroves during one or more of the reference periods
 203 considered. This results in a mangrove mask which we used to mask all other areas and compute the share

Table 2. Accuracy assessment of multitemporal land use and landcover classifications used for assessing the dynamics of mangrove vegetation in The Gambia between the period 2000 and 2020.

Land use and land cover class	2020-Classification		2010-Classification		2000-Classification	
	Consumers accuracy	Producer accuracy	Consumers accuracy	Producer accuracy	Consumers accuracy	Producer accuracy
Fresh waters	1.00	0.99	0.99	0.99	0.99	0.98
Salty waters	1.00	1.00	1.00	1.00	1.00	1.00
Closed forests	1.00	1.00	0.99	0.99	0.99	1.00
Open forests	0.97	0.97	0.97	0.97	1.00	0.99
Woody savannas	0.94	0.96	0.95	0.94	0.97	0.98
Savannas	0.97	0.97	0.96	0.93	0.98	0.97
Closed shrublands	0.98	0.97	0.94	0.94	0.95	0.91
Opened shrublands	0.97	0.96	0.94	0.93	0.90	0.93
Grasslands	0.99	0.98	0.96	1.00	0.98	0.98
Wetlands	0.99	0.99	0.96	0.98	0.97	0.98
Croplands	0.95	0.92	0.87	0.89	0.89	0.89
Built-up areas	1.00	0.99	1.00	1.00	1.00	0.99
Mosaics	0.92	0.96	0.89	0.87	0.88	0.89
Barren	0.98	1.00	0.99	0.99	0.98	0.99
Mangroves	0.99	1.00	1.00	0.99	1.00	1.00
Riperian vegetation	1.00	0.99	0.99	0.98	1.00	1.00
Overall accuracy		0.98		0.96		0.97
Kappa		0.98		0.96		0.96

204 of mangrove losses and gains in relation to other LULC. We then grouped these areas into 3 categories
 205 including areas where mangroves were converted into other LULC (decrease), areas where mangroves
 206 remained (stable), and areas where other LULC become mangroves (increase).

RESULTS

0.8 Classification accuracy

208 The classification accuracy was very strong, with a minimum value of 0.97 for both overall accuracy and
 209 Kappa coefficient (Table 2). Although we made the reference data comparable, the strong classification
 210 accuracy does not mean that every classification of LULC was perfect. There might be slight deviations
 211 due to numerous unforeseen factors.

0.9 Overall land use and land cover changes between 2000 and 2020

213 Change trajectory for the LULC types in The Gambia are presented in Table 3. Most of the predominant
 214 LULCs are on a declining trajectory e.g., closed forests, savannas, grasslands and wetlands experienced a
 215 significant decline in area. This is quite crucial because these are LULCs that do have strong connection
 216 with the predominant pastoral and agropastoral livelihood of the majority of the community in The
 217 Gambia. Mangroves, in a general made a significant gain with a total area gain of about 7784 ha over
 218 the 20 years period.

0.10 Tracing the sources of mangrove area dynamics in The Gambia

219 As per the current analysis, the mangrove area in The Gambia has improved during the period 2000-
 220 2020 (Table 4). The total area gain of mangroves in the period was about 11,951 ha (with almost 598
 222 ha per year). Mangroves gained land area mainly from wetlands, closed forests, barren areas and open
 223 shrublands close to the water bodies. It is important to also note that the gains vary. For instance, most
 224 of the reported area gains for mangroves are in Central River Region and around Kiang West National
 225 Park in Lower River Region where the ocean water that seasonally pushes more inland creates a space or
 226 mangrove expansion as other vegetation types retreat.

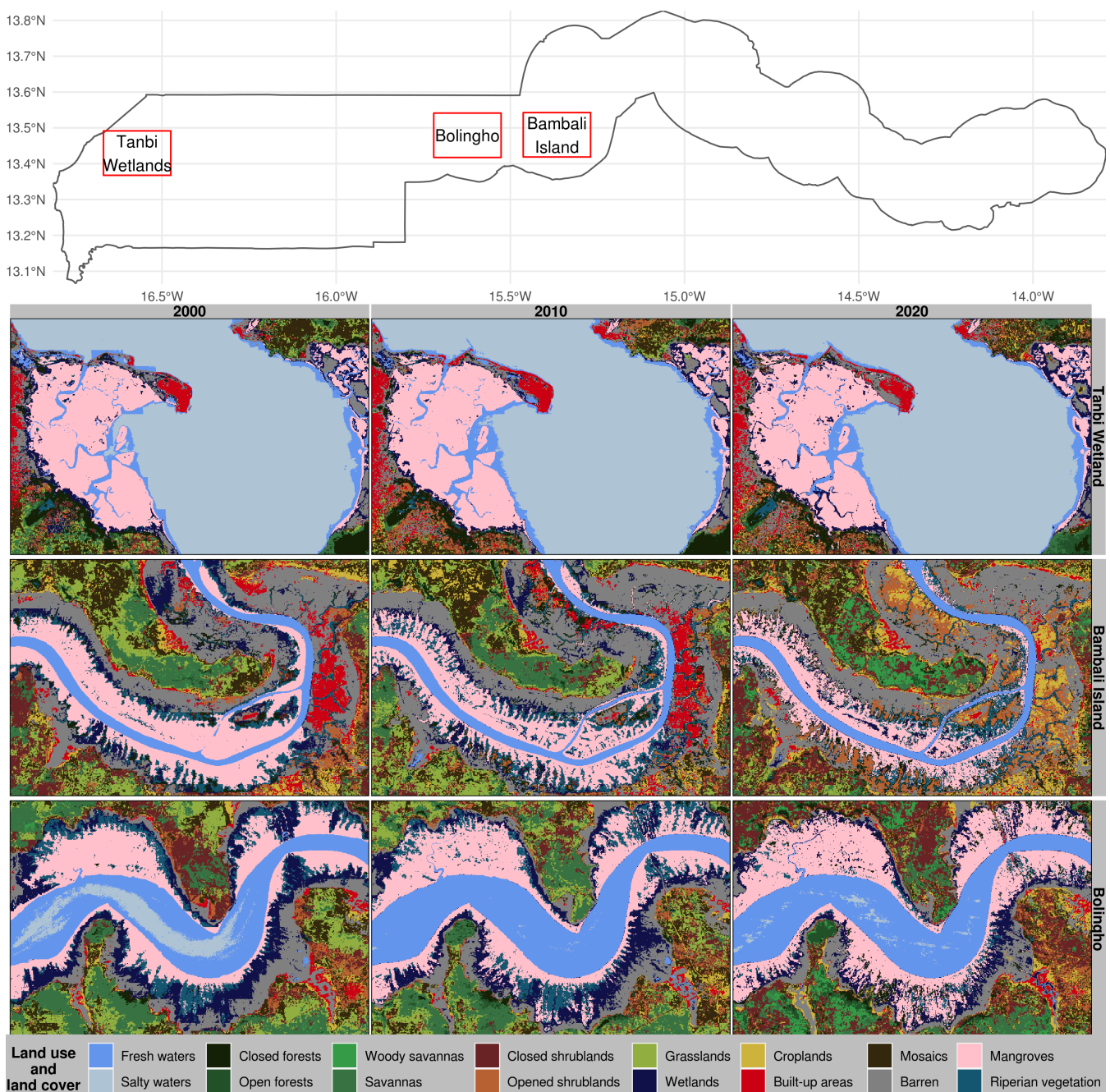


Figure 3. Dynamics of mangrove vegetation in The Gambia between the period 2000 and 2020.

227 During the same period, the loss in the existing mangrove vegetation area was estimated to be 4167 ha
 228 with an estimated annual loss of about 208 ha. The main LULC types threatening mangroves are open
 229 forests and woody savannas (especially in areas where water bodies are retreating), and crop lands and
 230 built-up areas (Table 4).

231 **0.11 Reflections on the change magnitudes and intensive change sites**

232 As also presented in Table 4, most of the mangrove area gains were recorded in the period 2010-
 233 2020. This could be largely attributed to growing awareness about the importance of this vegetation type
 234 for coastal area resilience and the livelihoods of thousands who depend on it (Moudingo et al., 2019;
 235 Feka and Morrison, 2017). Indeed, the growing restoration efforts in the country through the support of

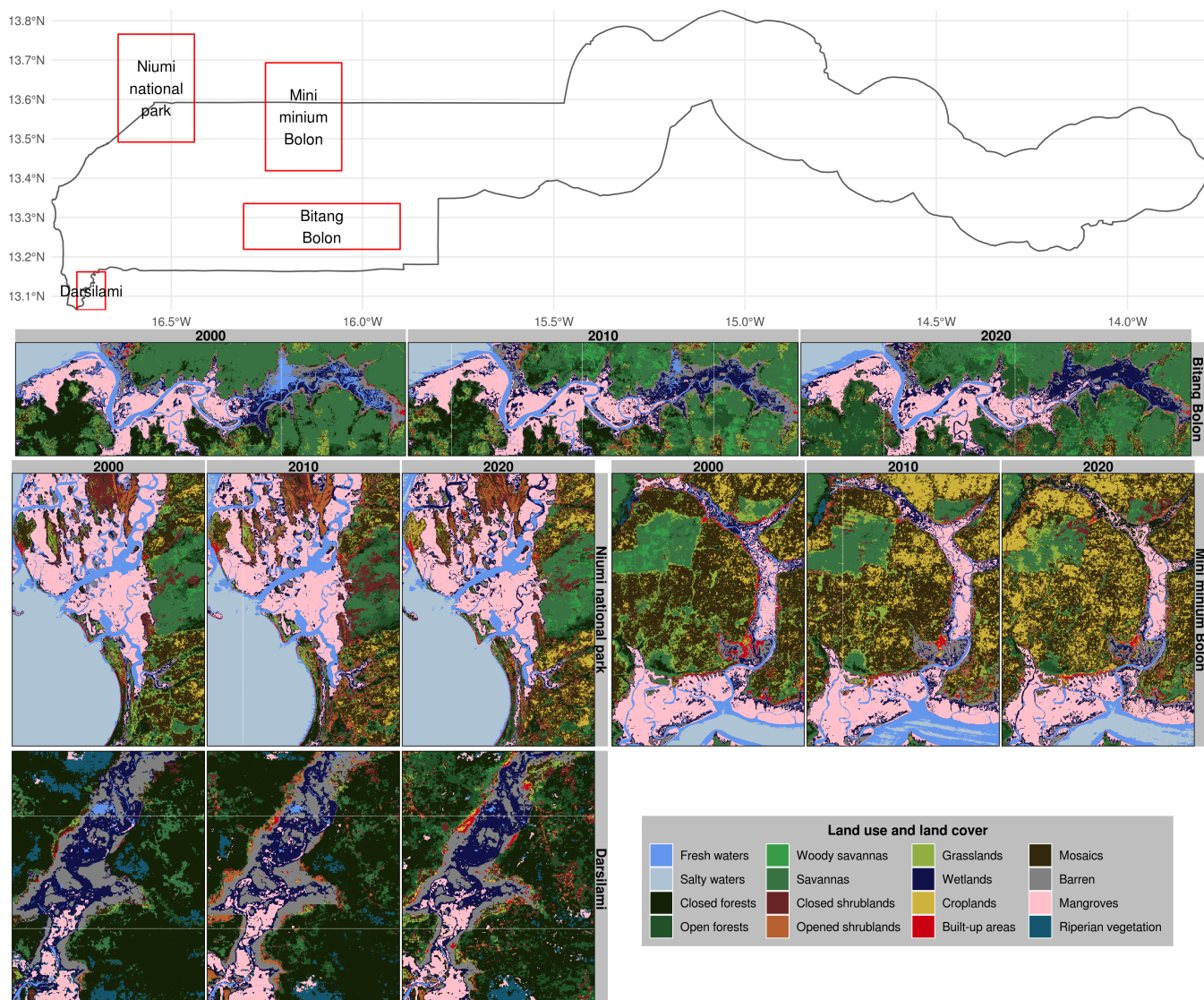


Figure 4. Dynamics of mangrove vegetation in The Gambia between the period 2000 and 2020.

236 multilateral and bilateral projects may have positively contributed to this increase. The main emphasis on
 237 the mangroves is, in fact, after the broad realization of the growing threats of climate change (e.g., sea
 238 level rise) on livelihoods and infrastructures which mangroves and other coastal vegetation could protect
 239 strongly.

240 It is important to note that net gains in mangrove does not necessarily mean there is no mangrove
 241 loss in the country. As presented earlier, the recorded loss is quite huge in relation to the investments
 242 needed to get such vegetations back to its full form through restoration. It is therefore necessary to
 243 emphasize the fact that the observed net gains should not mask the ongoing degradation of mangroves
 244 in different parts of the country. With the ongoing losses, the damage to livelihoods and biodiversity,
 245 such as fish and marine life, is significant. There still needs a strong push for minimizing the losses
 246 being recorded and invest in restoring those areas that are devoid of such vegetation already. As noted by
 247 Cormier-Salem & Panfili Cormier-Salem and Panfili (2016), the investments in reforestation of mangrove
 248 areas have made significant progresses on restoring the mangrove structure but in effect were not able to
 249 achieve the delivery of services and functions as anticipated. As the authors noted in case of Senegal, the

Table 3. Dynamics of major land use and land cover in The Gambia over 20 years period.

Land use and land cover class	2020	2010	2000	Change (2000-2020)
Fresh waters	34,146.64	39,470.47	34,790.69	-644.05
Salty waters	54,124.64	50,437.79	58,252.98	-4,128.34
Closed forests	61,875.77	83,280.79	86,139.19	-24,263.42
Open forests	81,347.26	30,991.32	12,212.32	69,134.94
Woody savannas	32,965.98	10,394.19	8,458.35	24,507.63
Savannas	114,013.80	151,760.70	164,881.50	-50,867.70
Closed shrublands	162,892.50	153,688.10	162,278.10	614.40
Opened shrublands	103,685.20	105,685.40	102,722.20	963.00
Grasslands	75,660.51	90,807.37	110,155.41	-34,494.90
Wetlands	30,199.09	36,001.28	37,022.08	-6,822.99
Croplands	67,007.38	64,509.15	42,938.62	24,068.76
Built-up areas	12,617.83	11,357.80	15,729.52	-3,111.69
Mosaics	199,673.30	190,552.80	198,782.60	890.70
Barren	42,568.52	46,921.99	37,602.37	4,966.15
Mangroves	59,144.58	58,860.63	55,140.37	4,004.21
Riperian vegetation	9,524.71	16,727.91	14,341.24	-4,816.53
Total	1,141,447.71	1,141,447.69	1,141,447.54	

Table 4. Results of the land use land cover changes and indications of where mangroves lost and gained in area in hectares.

Land use and land cover class	2000 - 2010		2010 - 2020		2000 - 2020	
	Gain	Loss	Gain	Loss	Gain	Loss
Fresh waters	338.65	224.16	68.93	95.47	490.84	247.56
Salty waters	0.00	0.00	0.00	0.00	0.09	0.00
Closed forests	406.42	100.13	386.59	1,624.66	473.74	1,309.45
Open forests	0.44	0.44	0.26	7.32	1.92	10.10
Woody savannas	0.00	0.00	0.00	0.00	0.44	0.70
Savannas	0.26	1.31	0.87	2.79	16.80	2.79
Closed shrublands	2.09	0.09	0.52	3.65	11.22	3.22
Opened shrublands	1.04	0.26	0.35	13.83	2.94	4.96
Grasslands	0.00	1.57	0.52	0.17	2.96	0.78
Wetlands	3,791.40	1,033.82	2,773.75	2,104.39	5,263.35	2,213.04
Croplands	0.00	0.26	0.26	1.04	0.09	1.04
Built-up areas	0.17	1.48	8.01	2.52	2.68	3.13
Mosaics	0.35	0.52	0.40	0.09	3.48	0.44
Barren	45.32	9.66	41.07	97.79	255.82	142.08
Riperian vegetation	2,531.87	2,024.08	2,608.22	1,652.08	3,146.91	1,729.76
Total	7,118.02	3,397.76	5,889.75	5,605.80	9,673.26	5,669.05

250 mangrove restoration was largely done in a campaign mode with emphasis on area rather than restoring
 251 the ecosystem goods and services from the mangroves.

252 Areas such as Allahein recorded significant losses as indicated in Figure 4 on the Gambia side, though
 253 it made gains on Senegal side interestingly. Though not confirmed, this probably could be due to differing
 254 measures taken by the countries whereby Senegal may be conserving and investing in the area while on the
 255 Gambia side there is a lot of land cover conversion happening for use as settlement and farming besides
 256 the booming near coast activities directly and indirectly affecting the mangroves. Though changes around
 257 Tanbi and Bulock areas do not seem to be significantly large, Tanbi has enjoyed the legislative support
 258 (i.e., being one of the wetland national parks in the country and has emphasis from the Department of
 259 Parks and Wildlife). Bulock, on the other hand, did not significantly face any major forces of change
 260 except basic extractive uses by communities around the mangroves.

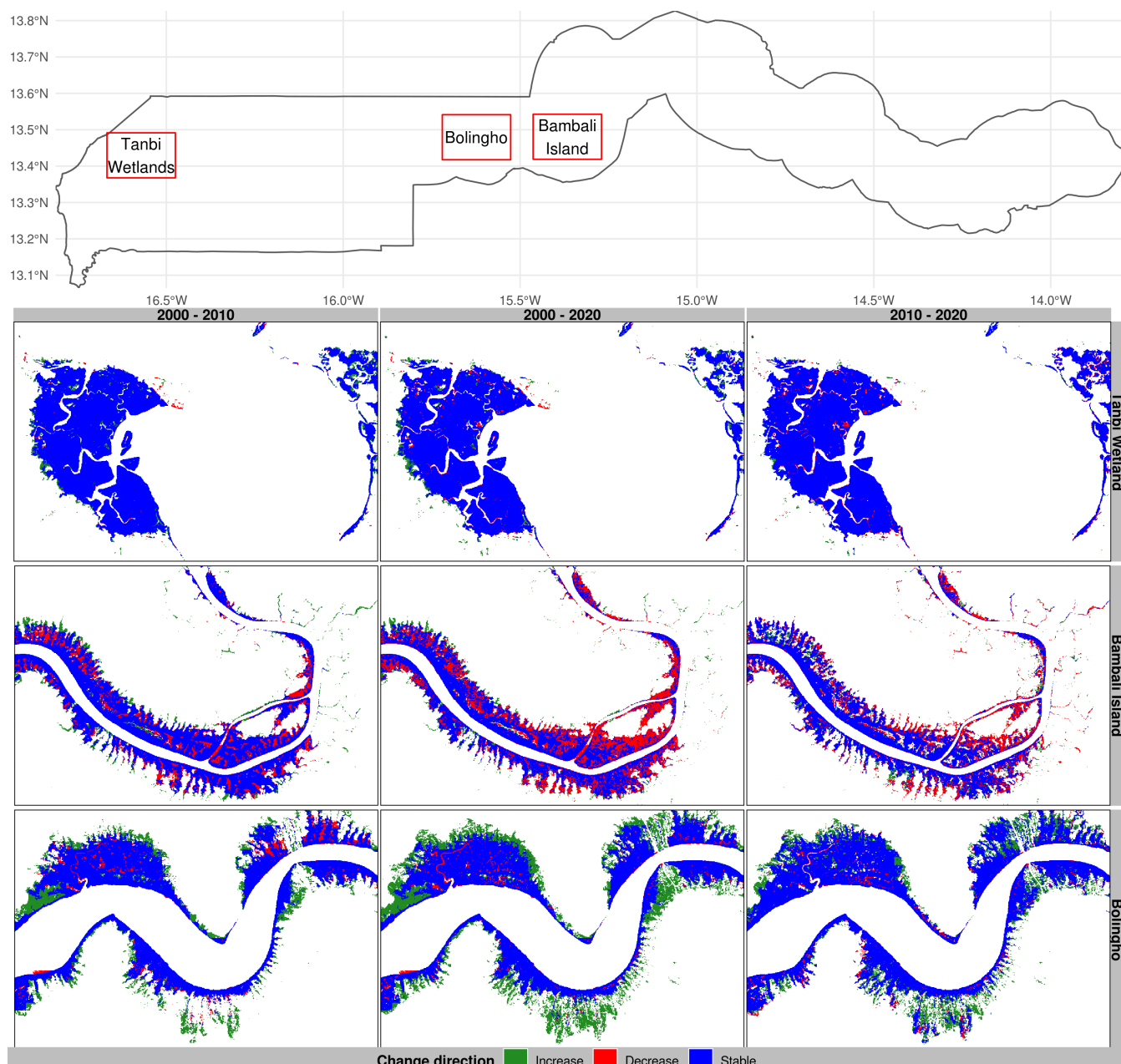


Figure 5. Dynamics of mangrove vegetation in The Gambia between the period 2000 and 2020.

DISCUSSION

DISCLOSURE/CONFLICT-OF-INTEREST STATEMENT

261 The authors declare that the research was conducted in the absence of any commercial or financial
 262 relationships that could be construed as a potential conflict of interest.

AUTHOR CONTRIBUTIONS

263 LD AND ILH contributed to conception and design of the study. JI and ILH organized the database. ILH
 264 performed the statistical analysis. JL and ILH wrote the first draft of the manuscript. ILH, JI, and LD
 265 wrote sections of the manuscript. All authors contributed to manuscript revision, read, and approved the
 266 submitted version.

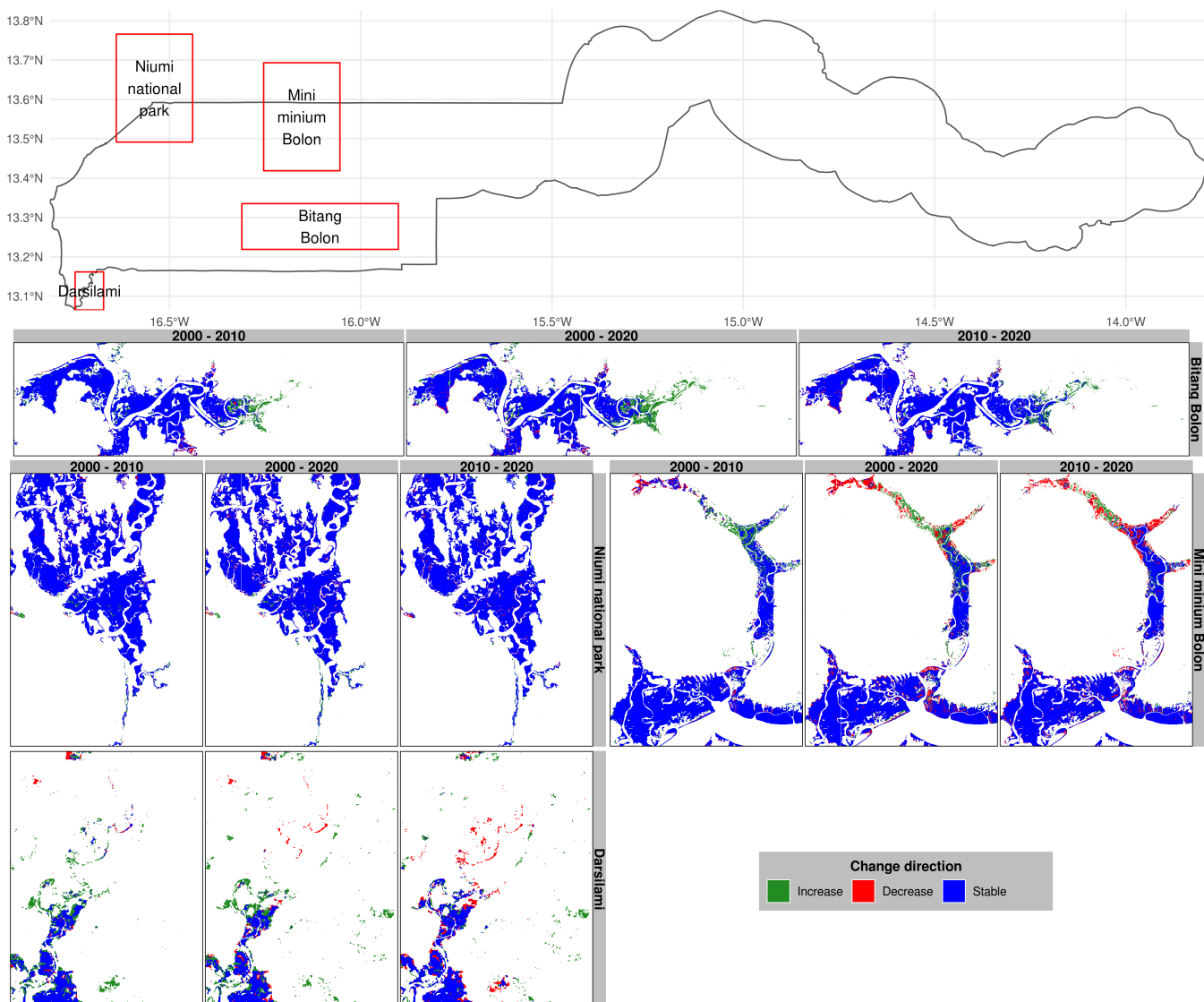


Figure 6. Dynamics of mangrove vegetation in The Gambia between the period 2000 and 2020.

ACKNOWLEDGMENTS

267 This study was funded by the World Agroforestry (International Centre for Research in Agroforestry;
268 ICRAF) under funding xxxxx contract Number 13016114. # References

1 SUPPLEMENTARY MATERIAL

2 DATA AVAILABILITY STATEMENT

269 We conducted the data analysis in Google Earth engine cloud computing platform (Gorelick et al.,
270 2017) and the R programming language (R Core Team, 2020). These were interfaced using rgee R
271 package (Aybar et al., 2020) which we used as bridge for throughput between Google Earth engine
272 and R . Both Google Earth engine and R are freely accessible (see <https://cran.r-project.org/index.html> for R and <https://code.earthengine.google.com/> for Google Earth
273 Engine). We automated the entire process, including the installation of the required R packages;
274 data processing; data streaming between Google Earth Engine and R; and results visualization, to
275 provide a complete reproducible workflow that could be adapted to other contexts. The replication files
276

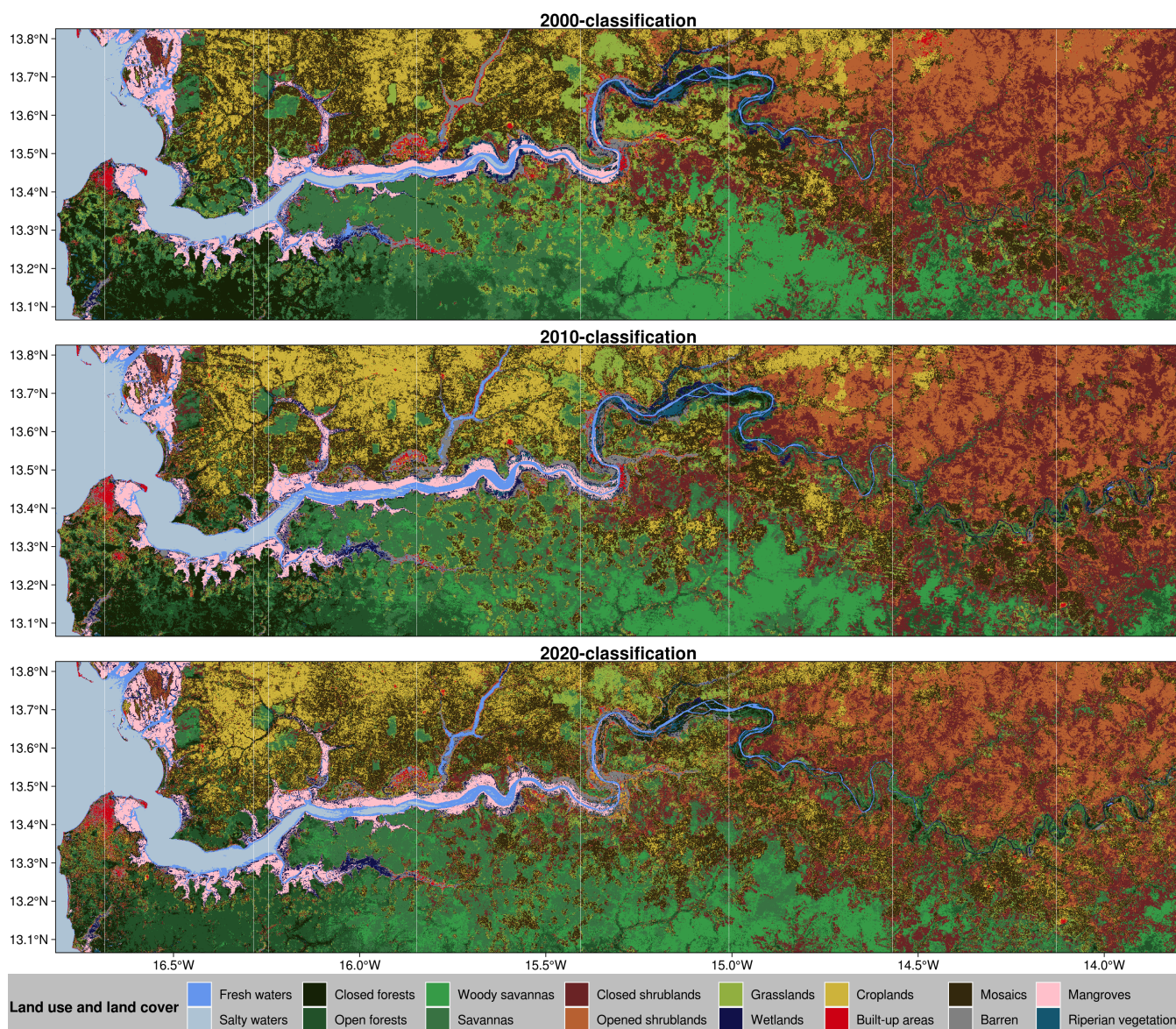


Figure 7. Land use and land cover classifications and changes based on continuous time series of monthly median composite of Landsat NDVI and NDWI acquired over the period 2000–2002 (2000-classification), 2010-classification and the period 2018–2020 (2020-classification) in The Gambia. These maps were derived by filling data gaps in the Landsat monthly composite using harmonic modelling after filling those gaps where MODIS NDVI and NDWI were available. Land use and land cover changes were estimated using image differencing.

277 along with further information for reproducing the work are available from <https://github.com/mangroveSpatial/mangroveGambiaReport>.
 278
 279 Ajonina, G., Diamé, A., and Kairo, J. (2013). Current status and conservation of mangroves in Africa: An
 280 overview. *Journal of Chemical Information and Modeling* 53, 1689–1699.
 281 Ali Bah, O. (2019). Land Use and Land Cover Dynamics in Central River Region of the
 282 Gambia, West Africa from 1984 to 2017. *American Journal of Modern Energy* 5, 5.
 283 doi:10.11648/j.ajme.20190502.11.

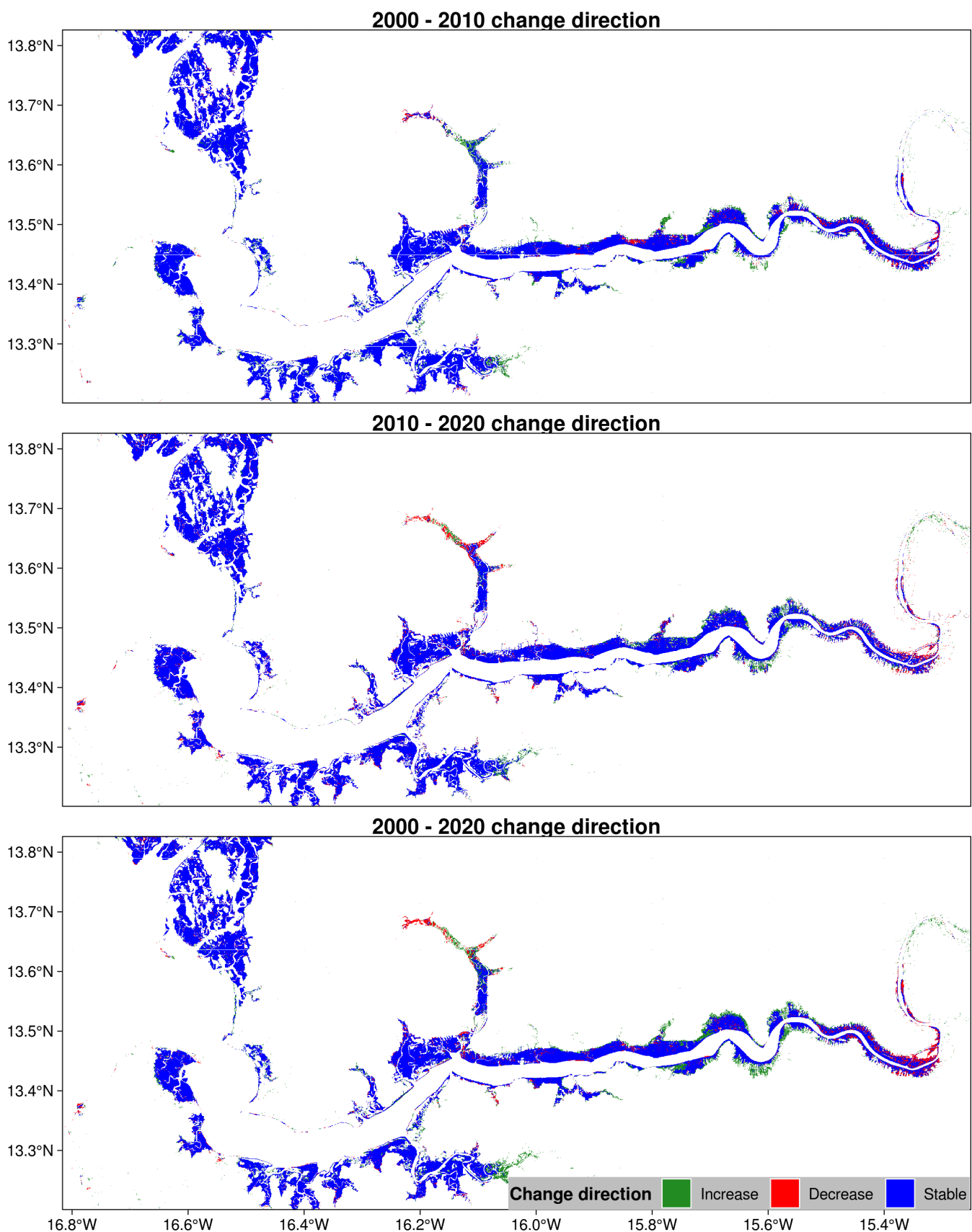


Figure 8. Dynamics of mangrove vegetation in The Gambia between the period 2000 and 2020.

- 284 Andrieu, J. (2018). Land cover changes on the West-African coastline from the Saloum Delta (Senegal) to
285 Rio Geba (Guinea-Bissau) between 1979 and 2015. *European Journal of Remote Sensing* 51, 314–325.
286 doi:10.1080/22797254.2018.1432295.
- 287 Aybar, C., Wu, Q., Bautista, L., Yali, R., and Barja, A. (2020). rgee: An R package for interacting with
288 Google Earth Engine. *Journal of Open Source Software* 5, 2272. doi:10.21105/joss.02272.
- 289 Ceesay, A., Hypolite Dibi, N., Njie, E., Wolff, M., and Koné, T. (2017). Mangrove Vegetation Dynamics
290 of the Tanbi Wetland National Park in The Gambia. *Environment and Ecology Research* 5, 145–160.
291 doi:10.13189/eer.2017.050209.
- 292 Cormier-Salem, M., and Panfili, J. (2016). Mangrove reforestation: greening or grabbing coastal
293 zones and deltas? Case studies in Senegal. *African Journal of Aquatic Science* 41, 89–98.
294 doi:10.2989/16085914.2016.1146122.
- 295 Di Gregorio, A., Henry, M., Donegan, E., Finegold, Y., Latham, J., Jonckheere, I., and Cumani, R. (2016).
296 *Land Cover Classification System: Classification concepts, Software version 3*. Rome, Italy: FAO.
- 297 Feka, N. Z., and Ajonina, G. N. (2011). Drivers causing decline of mangrove in West-Central Africa: A
298 review. *International Journal of Biodiversity Science, Ecosystem Services and Management* 7, 217–
299 230. doi:10.1080/21513732.2011.634436.
- 300 Feka, Z. N., and Morrison, I. (2017). Managing mangroves for coastal ecosystems change: A decade and
301 beyond of conservation experiences and lessons for and from west-central africa. *Journal of ecology*
302 and the natural environment 9, 99–123.
- 303 Fent, A., Bardou, R., Carney, J., and Cavanaugh, K. (2019). Transborder political ecology
304 of mangroves in Senegal and The Gambia. *Global Environmental Change* 54, 214–226.
305 doi:10.1016/j.gloenvcha.2019.01.003.
- 306 FRA (2000). Forest cover mapping and monitoring with NOAA - AVHRR and other coarse spatial
307 resolution sensors. Rome, Italy: FAO; FAO Available at: <http://www.fao.org/forestry/4031-0b6287f13b0c2adb3352c5ded18e491fd.pdf>.
- 309 Gorelick, N., Hancher, M., Dixon, M., Ilyushchenko, S., Thau, D., and Moore, R. (2017). Google Earth
310 Engine: Planetary-scale geospatial analysis for everyone. *Remote Sensing of Environment* 202, 18–27.
311 doi:10.1016/j.rse.2017.06.031.
- 312 Moudingo, J.-H. E., Ajonina, G., Eugene, D. M., Jarju, A. K., Jammeh, K., Conteh, F., Taal, S.,
313 Touray, L. M., Njei, M., and Janko, S. (2019). “Enhancing Resilience of Vulnerable Coastal
314 Areas and Communities: Mangrove Rehabilitation/Restoration Works in the Gambia,” in *Handbook*
315 of environmental materials management (Cham: Springer International Publishing), 2647–2691.
316 doi:10.1007/978-3-319-73645-7_68.
- 317 R Core Team (2020). *R: A language and environment for statistical computing*. Vienna, Austria: R
318 Foundation for Statistical Computing Available at: <https://www.R-project.org/>.
- 319 Roy, D. P., Kovalskyy, V., Zhang, H. K., Vermote, E. F., Yan, L., Kumar, S. S., and Egorov, A. (2016).
320 Characterization of Landsat-7 to Landsat-8 reflective wavelength and normalized difference vegetation
321 index continuity. *Remote Sensing of Environment* 185, 57–70. doi:10.1016/j.rse.2015.12.024.
- 322 Satyanarayana, B., Bhanderi, P., Debry, M., Maniatis, D., Foré, F., Badgie, D., Jammeh, K., Vanwing,
323 T., Farcy, C., Koedam, N., et al. (2012). A socio-ecological assessment aiming at improved forest
324 resource management and sustainable ecotourism development in the mangroves of Tanbi Wetland
325 National Park, the Gambia, West Africa. *Ambio* 41, 513–526. doi:10.1007/s13280-012-0248-7.
- 326 Shumway, R. H., and Stoffer, D. S. (2011). *Time Series Analysis and Its Applications*. Third edit. New
327 York, NY: Springer New York doi:10.1007/978-1-4419-7865-3.

- 328 Spalding, M., Blasco, F., and Field, C. (1997). *World Mangrove Atlas*. Okinawa, Japan: The International
329 Society for Mangrove Ecosystems.
- 330 The Gambia Bureau of Statistics (2012). The Gambia 2013 Population and Housing Census
331 Preliminary Results. The Gambia Bureau of Statistics; The Gambia Bureau of Statistics
332 Available at: [http://statsghana.gov.gh/gsscommunity/adm_program/modules/](http://statsghana.gov.gh/gsscommunity/adm_program/modules/downloads/get_file.php?file_id=27)
333 [downloads/get_file.php?file_id=27](http://statsghana.gov.gh/gsscommunity/adm_program/modules/downloads/get_file.php?file_id=27).
- 334 UNEP (2007). Mangroves of Western and Central Africa. Cambridge, UK: UNEP; UNEP-WCMC,
335 UNEP Available at: <https://archive.org/download/mangrovesofweste07corc/>
336 [mangrovesofweste07corc.pdf](https://archive.org/download/mangrovesofweste07corc.pdf).
- 337 Vermote, E. (2015). MOD09A1 MODIS/Terra Surface Reflectance 8-Day L3 Global 500m SIN Grid
338 V006 [Data set]. Available at: <http://doi.org/10.5067/MODIS/MOD09A1.006> [Accessed
339 June 6, 2021].
- 340 Wulder, M. A., Loveland, T. R., Roy, D. P., Crawford, C. J., Masek, J. G., Woodcock, C. E.,
341 Allen, R. G., Anderson, M. C., Belward, A. S., Cohen, W. B., et al. (2019). Current status
342 of Landsat program, science, and applications. *Remote Sensing of Environment* 225, 127–147.
343 doi:10.1016/j.rse.2019.02.015.
- 344 Zhu, Z., and Woodcock, C. E. (2014). Continuous change detection and classification of
345 land cover using all available Landsat data. *Remote Sensing of Environment* 144, 152–171.
346 doi:10.1016/j.rse.2014.01.011.